Hydrology Research

Hydrology Research Vol 54 No 2, 265 doi: 10.2166/nh.2023.129

Comparative analysis and risk assessment of dam-break floods: Taking Pingshuijiang Reservoir as an example

Xun Jiang[a], Jie Meng[b], Bingjie Fan[c], Chongxu Zhao[d,e,*], Yanshuang Zheng[d,e], Qianlu Xiao[d,e], Chunjin Zhang[d,e] and Dongfang Ma[d,e]

[a] Zhejiang Design Institute of Water Conservancy and Hydro-Electric Power Co., Ltd, No. 66 Funing Lane, Shangcheng District, Hangzhou 310000, China
[b] Zhejiang Yugong Information Technology Co., Ltd, T2-3A, Horui Science Park, Changhe Street, Binjiang District, Hangzhou 310000, China
[c] Shanxi Yellow River Flexible Flood Proofing Emergency, No. 4738, Sushui East Street, Yuncheng Economic and Technological Development Zone, Yuncheng 044000, China
[d] Yellow River Institute of Hydraulic Research, Yellow River Conservancy Commission, No. 45 Shunhe Road, Zhengzhou 450003, China
[e] Key Laboratory of Lower Yellow River Channel and Estuary Regulation, MWR, Zhengzhou 450003, China
*Corresponding author. E-mail: charles_zcx@163.com

CZ, 0000-0002-7060-2109

ABSTRACT

Due to the huge potential energy associated with water storage in reservoirs, dam-break floods are often catastrophically destructive for people and structures downstream. This study aims to simulate and compare floods generated under various dam-break scenarios and their downstream impacts, taking Pingshuijiang Reservoir in southeastern China as an example. A two-dimensional hydrodynamic model is used to simulate the downstream evolution of floods under three dam-break scenarios, and the breach flood and downstream inundation process are analyzed. Gradual failure of the main dam leads to near-total inundation of the nearby town over c. 1 h, allowing time for warning and evacuation. Instantaneous failure of the main dam results in larger peak flow, greater submergence depth and faster inundation (20 min), leaving little time for warning/evacuation. Instantaneous failure of the auxiliary dam generates a much lower peak flow magnitude and, although the town is still largely submerged within 45 min, the shallow water depth and low velocity are conducive to rescue/evacuation. The results show significant variation in flood process and submergence due to dam size and failure mode that provide guidance for dam-break flood risk assessment and disaster avoidance planning.

Key words: dam-break discharge, dam-break flood, dam-break scenario, flood routing, Pingshuijiang Reservoir

HIGHLIGHTS

- Simulate and compare floods generated under various dam-break scenarios and their downstream impacts.
- The results will provide guidance for dam-break flood risk assessment and disaster avoidance planning.

GRAPHICAL ABSTRACT

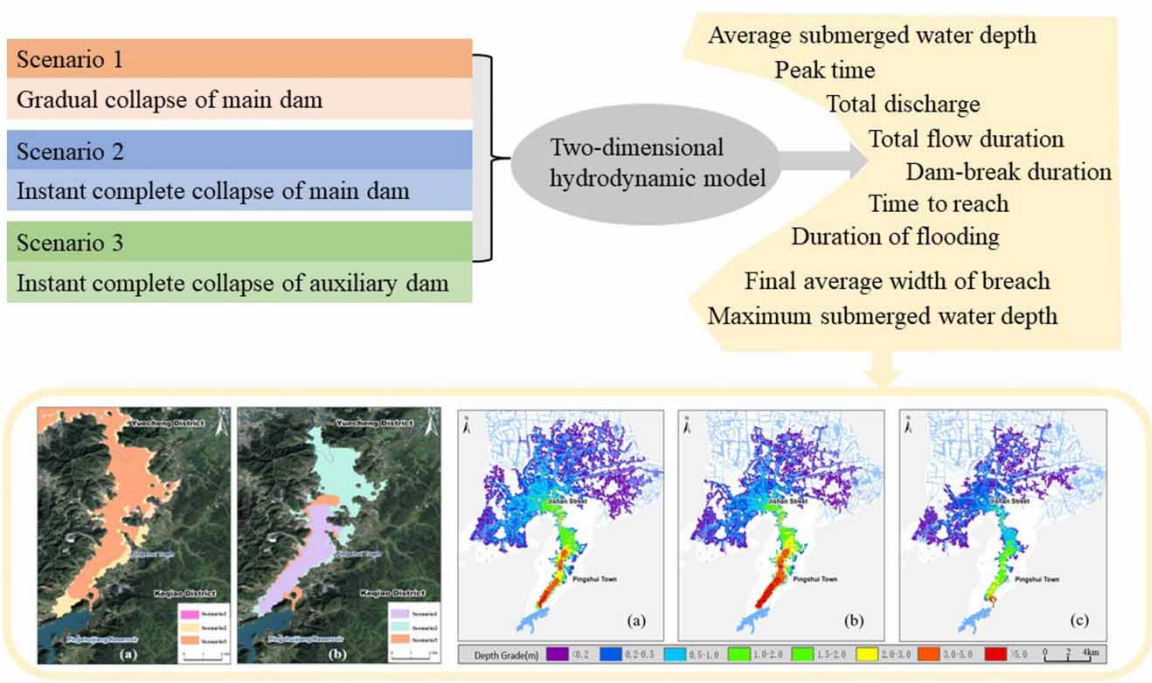

INTRODUCTION

Construction of reservoir dams and other water conservancy projects can deliver many social and economic benefits, such as flood control, power generation, irrigation, water supply, fishery, tourism, etc. (Safarzadeh 2017; Guo *et al.* 2019; Khoshkonesh *et al.* 2022). However, the huge potential energy generated by flood storage also poses a great threat to the safety of life and property of people living downstream (Xu *et al.* 2021). In recent years, the increased frequency of extreme climate phenomena (Alcayna *et al.* 2022) has put the reservoir flood control standards calculated and formulated using existing hydrological data under scrutiny (Chen & Sun 2021). Climate extremes also lead to the operation of reservoir dams under adverse conditions for a longer time, which directly affects the stability of the dam structure and accelerates ageing of hydraulic materials (Cai *et al.* 2011), enhancing the dam-break potential.

Evidence from historical dam-break events in various countries highlights the potential for catastrophic damage to downstream people and properties (Qiu *et al.* 2021; Seiya *et al.* 2021). One of the most significant dam-break events in China was on 8 August 1975, the collapse of the Banqiao Reservoir dam in western Henan province due to extreme rainfall generated by a tropical cyclone. The resulting floods affected 11 million people across 29 counties, with more than 26,000 deaths, 5.96 million houses destroyed, 11,300 km^2 of farmland inundated, 302,300 livestock lost and 102 km of the Beijing-Guangzhou railway destroyed; direct economic losses of nearly 10 billion yuan were recorded (Bai & Zhen 2014). The Banqiao event involved a complete dam collapse, but even partial collapses can have devastating impacts due to chain effects. On 19 May 2020, the flood wave generated by the partial failure of the Edenville dam in Michigan in the United States led to overtopping of the Sanford dam and Poseyville embankment downstream, resulting in more than 10,000 people having to evacuate their homes and damage to more than 2,000 homes, as well as multiple roads, bridges and businesses (Pradel & Lobbestael 2021).

Dam failure is mostly caused by floodwater infiltration, overtopping, material instability or external damage. The dam failure process may be gradual or instantaneous; the nature of dam failure (partial or complete, gradual or instantaneous) influences the flood process and downstream impacts. Instantaneous failures are often associated with catastrophic downstream impacts, such as the 1959 dam-break dam-break at Malpasset in France (Duffaut & Larouzée 2019) and the 2011 Fujinuma dam-break in Japan (Pradel *et al.* 2017). Systematic analysis of different dam-break modes requires the determination of flood parameters such as peak flow, time to peak, velocity and area of inundation.

Numerous approaches to modeling dam-break flood parameters and risk have been published in recent years. Delenne *et al.* (2012) assessed the potential of local sensitivity analysis for the analysis of uncertainty with respect to flash flood and dam failure risks in river hydrodynamics. Seyedashraf *et al.* (2018) used a method based on computational intelligence systems to simulate the classical one-dimensional dam-break flow problem that addresses the shortcomings of existing analytical and numerical models. Tedla *et al.* (2021) used hourly hydrological and meteorological data as well as high-resolution land surface datasets to simulate design floods for piping dam failure with empirical dam breach methods. With the requirements of decision makers for high-precision flood prediction, identification of flood-prone areas, flood inundation mapping and inundation assessment, GIS, high-definition remote sensing images, high-precision digital elevation model (DEM), MIKE software and The Hydrologic Engineering Center – River Analysis System (HEC-RAS) have gradually been added to dam-break numerical modeling (Alvarez *et al.* 2017; Mao *et al.* 2017; Enea *et al.* 2018; Tamm & Tamm 2020; Mudashiru *et al.* 2021). A recent example is the work of Li *et al.* (2021) who used high-precision topographic mapping and DEM of the area around Qianping Reservoir in Ruyang County, Henan Province, China as the basis for one- and two-dimensional coupled dam-break numerical models using Geographic Information System (GIS) technology and MIKE software. Li *et al.* (2021) simulated the dam-break and flood discharge process under the 5000-year check flood level, calculated the flow process of the reservoir dam-break and the downstream evolution of the flood, obtaining flood risk information such as submerged area and flow patterns. Weilian *et al.* (2021) revealed the deficiencies of the existing systems for the floods simulation: the input data parameters are complex and the simulation process is cumbersome and time consuming. Then they developed a platform for the rapid 3D reproduction of dam-break floods which supports rapid reproduction at different times and positions. Based on Monte Carlo Simulation (MCS), HEC-RAS 2D, and HEC-LifeSim models, EL Bilali Ali *et al.* (2022) proposed an integrated approach on dam-break simulation, which can deal with the flood risk with probability rather than analyzing a few dam-break scenarios.

Most existing research focuses on a single dam-break scenario, and there is a lack of comparative analysis of flood process and downstream impact under different dam-break scenarios. Given the numerous potential causes of dam failure, there is potential for great differences in flood flow and downstream evolution with different dam-break scenarios. Single-scene dam-break flood analysis cannot fully meet the needs of practical applications; it is important to study the flood propagation process and downstream effects under various dam-break scenarios. This study explores the flood discharge and evolution process under three typical dam-break scenarios. Characteristic parameters such as breach flow, outflow time, time to peak, submerged range, flood velocity and flood arrival time are compared and analyzed for each scenario, and the disaster implications for downstream peoples and the structures are evaluated. The results are of significance for reservoir management departments to formulate flood control emergency plans, analyze flood risks and provide decision support for emergency agencies. The work also has reference value for government to improve regional flood control and disaster reduction capabilities and to enhance people's awareness of risk avoidance.

STUDY AREA AND DATA

This study uses Pingshuijiang Reservoir, a medium-sized reservoir in the economically developed coastal region of southeastern China, as a case study to model flood response to three dam-break scenarios. The reservoir is located in Keqiao District, Shaoxing City, Zhejiang Province, China (Figure 1).

Pingshuijiang Reservoir is in the upper reaches of Pingshui River, within the Cao'e River Basin, at the northern foot of Kuaiji Mountain. The reservoir is vulnerable to severe weather associated with plum rain (July to August rainy season) and typhoons that increase the risk of dam failure. Directly downstream of the reservoir are the populous and economically developed areas of Kecheng Pingshui Town and Yuecheng District (Figure 2). In 2020, Keqiao District had a permanent population of 1.1 million and Gross Domestic Product (GDP) of 151.7 billion yuan, while the permanent population of Yuecheng District was 1.02 million and its GDP 100.9 billion yuan. Therefore, there is a high potential for dam-break flooding to cause a serious disaster.

Pingshuijiang is a medium-sized reservoir with comprehensive functions of flood control, irrigation, water supply and power generation. The dam site is about 20 km from Shaoxing City, along the main stem of the Pingshui River. The river is a mountain system, with short and scattered tributaries. Floods are mainly generated by typhoon rainstorms and plum rain, which rise and fall rapidly and generally last for about 3 days. For dam-break floods, the potential area influenced

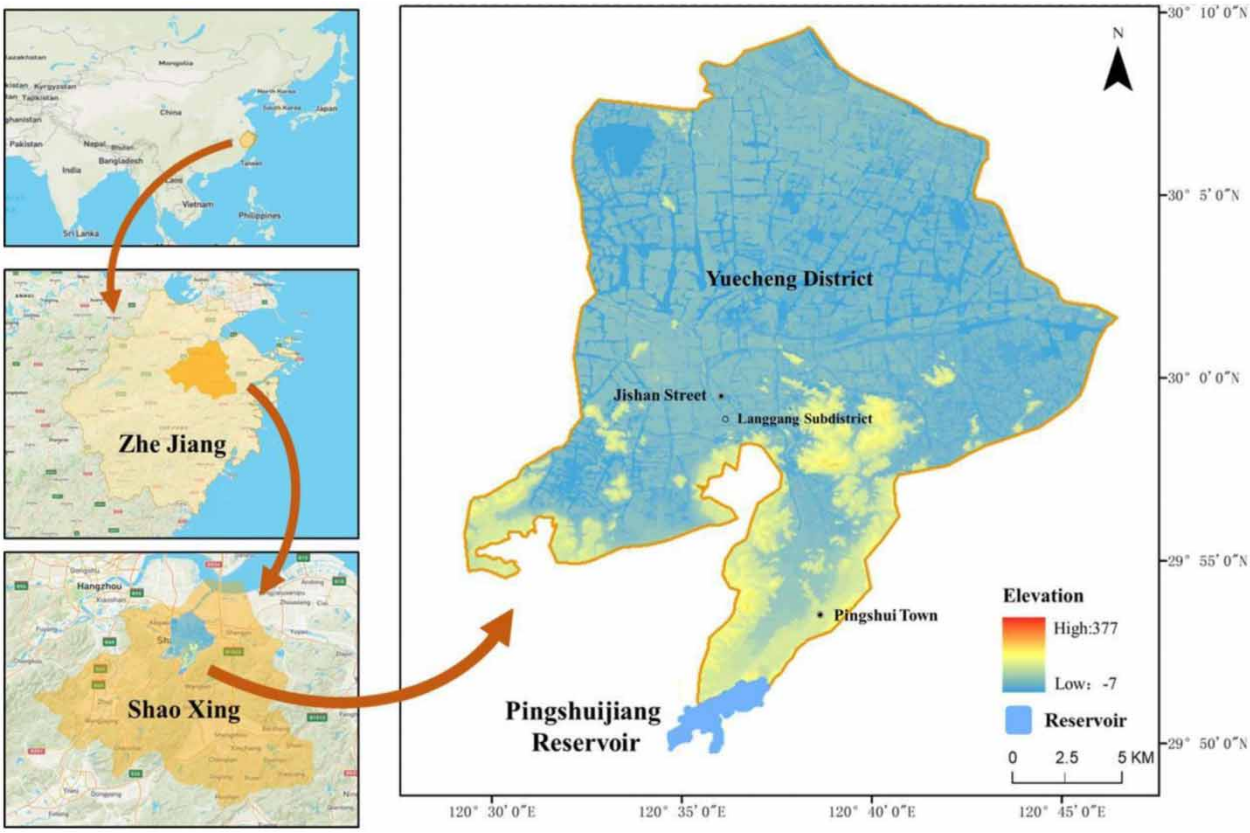

Figure 1 | Location of Pingshuijiang Reservoir, southeastern China, showing topography of downstream area.

downstream is about 357 km^2, including Pingshui Town and Yuecheng District. The northern part of the reservoir is adjacent to Pingshui Town, which is in a basin and is surrounded by mountains. If a dam-break occurs, flood waters can only be discharged through the Kuaijishan gorge in the northern part of the town, and are directed to the Jishan Street area of Yuecheng District. This kind of reservoir is common in the economically developed areas of the Yangtze River Delta. It is of great significance to study the dam-break flood of this kind of reservoir for the safety risk analysis of the whole Yangtze River Delta region.

A range of data sources were used in the study to provide input for the simulation, including information on terrain and reservoir parameter characteristics. For terrain data, a 2×2 m DEM data of Shaoxing City was utilized. The layer structure of the basic risk map geographic information database was established using the spatial database of ArcGIS, and the processed DEM and related data were then constructed. The database coordinate system is CGCS2000, on the Gauss–Kruger projection, and the elevation reference is the China national elevation datum 1985. Baseline information on reservoir and dam characteristics was obtained from the Pingshuijiang Reservoir Control Operation Plan, as shown in Table 1.

METHODS

A dam-break flood model was constructed to determine the breach flood process and downstream evolution of the flood wave. The model has two elements: the breach flow process and the flood routing process.

It is necessary to first determine the breach flow process as it provides the upper boundary condition of the flood routing model. The gradual dam-break process needs to be deduced first. In the case of uniform development of the breach, the process line of the breach width B can be determined as follows:

$$B = B_0 + (B_m - B_0)t/T_f \quad (1)$$

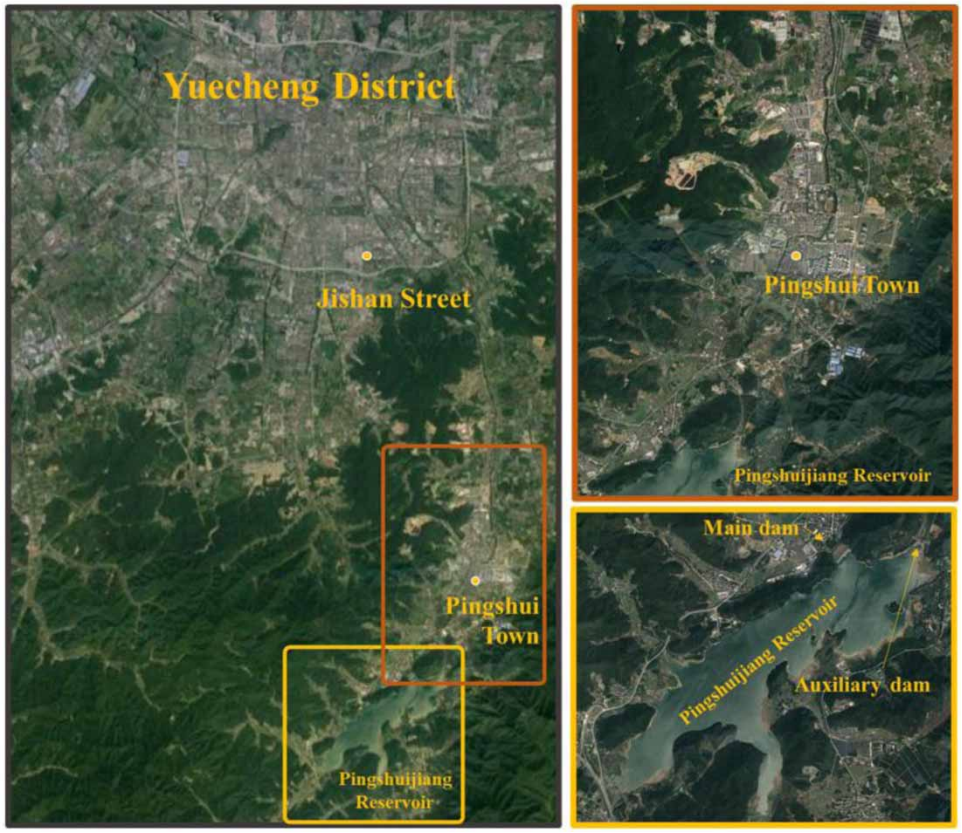

Figure 2 | Relationship between Pingshuijiang Reservoir and Pingshui Town, Yuecheng District.

Table 1 | Characteristics of Pingshuijiang Reservoir

Total capacity (m^3)	Design flood water level (m)	Main dam crest elevation (m)	Average length of main dam (m)	Maximum height of main dam (m)	Auxiliary dam crest elevation (m)	Average length of auxiliary dam (m)	Maximum height of auxiliary dam (m)
5,457	48.25	51.1	230	30.5	51.5	74	12.8

In Equation (1): B_0 is the initial breach width, here taken as 20 m; B_m is the final breach width (m), which can be calculated using the Lu Jikang empirical formula of the China Institute of Water Resources and Hydropower Research, see Equation (2); t is duration (s); T_f is the duration of breach development (s), which can be deduced by Equation (3):

$$B_m = 0.1803KV_r^{0.32}H_b^{0.19} \tag{2}$$

In Equation (2): B_m is the average width of the final breach (m); H_b is the effective height of the burst (m); V_r is the effective discharge capacity of the reservoir (m^3); K is the correction coefficient, here taken as 1:

$$T_f = 0.00245KV_r^{0.53}H_b^{-0.9} \tag{3}$$

Considering the most unfavorable situation where the breach develops vertically to the bottom of the dam and develops at a uniform speed, the longitudinal development process of the breach can be obtained by analogy using Equation (1).

The dam breach development process can be obtained through Equations (1)–(3). Assuming that the inflow flow in the process is 0, the breach flow at any time can be calculated by the Schocklich empirical formula:

$$Q = \frac{8}{27} g^{0.5} (B/b)^{0.25} b H_0^{1.5} \tag{4}$$

where Q is the breach flow (m^3/s); B is the dam crest length (m); b is the breach width (m); H_0 is the water depth of the breach (m).

The discharge of the auxiliary dam spillway of Pingshuijiang Reservoir is calculated by the weir flow equation:

$$Q = \sigma \theta m b (2g)^{0.5} H^{1.5} \tag{5}$$

where σ is the submergence coefficient; θ is the lateral contraction coefficient; m is the weir flow coefficient; b is the crest width (m); H is the water head (m).

For flood routing, the MIKE21 two-dimensional hydrodynamic calculation model was used to simulate the flood evolution and inundation process downstream of the reservoir. The model generalizes the flood-affected area, using a triangular mesh as the basis for simulation. As Pingshui Town as the key research object, the mesh was encrypted. The 357 km^2 area was divided into 69,253 grids cells, with terrain data use to assign the grid elevation. The upper boundary of the model was set at Pingshuijiang dam site or the auxiliary dam site, according to the scheme chosen for simulation. The lower boundary was set using closed features such as Shaozhu Expressway, Cao 'e River and Sanjiang River. The calculation time step was set as 1 min, and the flood routing process was determined over 36 h.

Scenario setting

Failure of earth-rock dams may be gradual, due to flood infiltration and overtopping, or instantaneous, for example, due to strong external damage. Based on the regional background, engineering status and external factors, three dam-break scenarios for the design flood level (48.25 m) were formulated and compared for Pingshuijiang Reservoir. Details of each scenario are given in Table 2 and outlined below:

(1) Gradual collapse of the main dam. As the water gradually rises to the design flood level during the event, water penetrates and erodes the main dam, resulting in its gradual collapse. This generates a large discharge flood in a short time. The upper boundary of the model is set as the breach flow process at the main dam site.
(2) Instantaneous complete collapse of the main dam. This scenario considers the case where the reservoir is at the design flood level and is affected by strong destructive factors, such as earthquake activity or war, so that the main dam fails instantaneously. This results in a huge discharge flood in a very short time. The upper boundary of the model is set as the breach flow process at the main dam site. Due to the rapidity, there is no need to consider the breach development process in this scenario. The average width of the dam is 230 m, and the flow process after dam-break can be calculated directly using Equations (4) and (5).
(3) Instantaneous complete collapse of auxiliary dam. This scenario considers the case where the water level is at the design flood level, but there is continued rainfall that may lead to flooding, so the auxiliary dam is artificially blown up to speed up flood discharge and ensure the safety of the main reservoir. This results in a small discharge flood in a very short time. The upper boundary of the model is set as the breach flow process at the auxiliary dam site. The average width of the auxiliary dam breach is 74 m.

Table 2 | Scenarios used in dam-break modeling

Number	Scenario	Example cause of dam-break	Flood characteristic
Scenario 1	Gradual collapse of main dam	Flood infiltration erosion	Large flow in a short time
Scenario 2	Instant complete collapse of main dam	Earthquakes, wars, etc.	Huge flow in a very short time
Scenario 3	Instant complete collapse of auxiliary dam	Artificial explosion	Relatively small flow in a very short time

RESULTS AND DISCUSSION

Dam-break discharge process

The dam-break process was simulated under the three dam-break scenarios. In Scenario 1, discharge starts low, increases to a peak, then falls gradually (Figure 3(a)). The initial flow mainly comes from spillway discharge, and flow gradually increases as the breach develops. Breach flow reaches 510 m^3/s at 15 min after initial dam dam-break, and then increases significantly to a peak of 11,440 m^3/s at 87 min. At peak flow, breach width reaches a maximum of 97 m. After the peak, with the decrease of reservoir water level, the discharge gradually decreases. The duration of the complete flood process is 249 min.

In Scenario 2, flood discharge peaks in the initial stage at 29,632 m^3/s, with a spillway discharge of 485 m^3/s (Figure 3(b)). The huge flow magnitude causes the reservoir water level to drop rapidly so that 10 min after the dam-break, water level is lower than the elevation of the spillway, and flood discharge from the spillway ceases. After about 30 min, discharge is around 9,000 m^3/s and then gradually decreases to 111 min when the event is essentially completed.

Under Scenario 3, all floodwater is dumped at the auxiliary dam and discharge peaks at 2,589 m^3/s at the initial stage (Figure 3(c)). Due to the relatively small discharge, flood duration is significantly longer (780 min), and the final reservoir water level is maintained at 38.7 m, which is the bottom elevation of the auxiliary dam.

The flood characteristics for each dam-break scenario are summarized in Table 3, and changes in water level and discharge over time are compared in Figure 4. The peak dam-break flood discharge under the scenarios 1, 2 and 3 is 11,440, 30,117 and 2,589 m^3/s, respectively. The instantaneous full failure of the main dam in Scenario 2 produces the highest peak discharge, 2.6 times greater than that of Scenario 1 and 11.6 times greater than Scenario 3. The time to peak is the longest in Scenario 1, the gradual failure of the main dam, at around 87 min after the dam-break. In Scenarios 2 and 3, instantaneous complete dam failure, the dam-breaks completely at the initial time and there is no further breach development. Hence, in Scenarios 2 and 3, flood discharge peaks at the start of the dam-break and gradually decreases with reservoir water level.

Flood duration in Scenarios 1, 2 and 3 is 249, 111 and 780 min, respectively. The longest flood duration is associated with instantaneous failure of the auxiliary dam (Scenario 3), which is 3.1 times that of Scenario 1 and 7 times that of Scenario 2. The main reason for this is the relatively small breach of the auxiliary dam, which allows only small volumes of outflow and the flood takes longer to be fully discharged.

Flood impact analysis

Based on the breach flow of each Scenario, combined with MIKE21 model analysis, the inundation range and downstream flood process were derived. The main characteristics of flood inundation under each Scenario are shown in Table 4. The

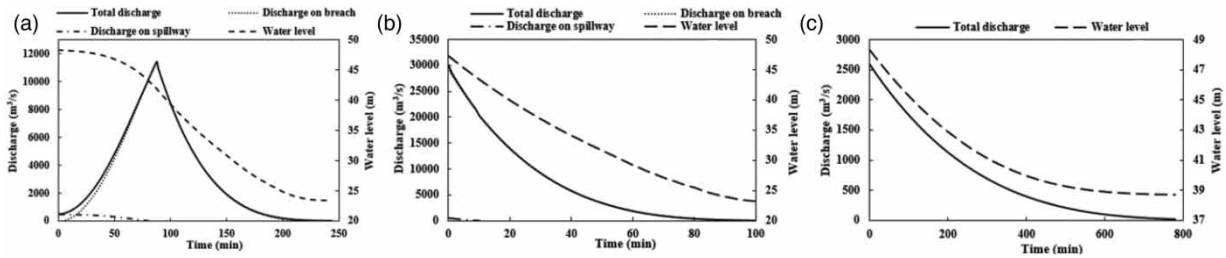

Figure 3 | Discharge and water level process for dam-break. (a) Scenario 1; (b) Scenario 2; (c) Scenario 3.

Table 3 | Flood characteristics of each dam-break scenario (see Table 2 for details of scenarios)

Scenario	Q_{max} (m^3/s)			Peak time (min)	Total flow duration (min)	Dam-break duration (min)	Final average width of breach (m)
	Breach	Spillway	Total				
Scenario 1	11,440	485	11,440	87	249	87	97
Scenario 2	29,632	485	30,117	1	111	0	230
Scenario 3	2,589	2,589	2,589	1	780	0	74

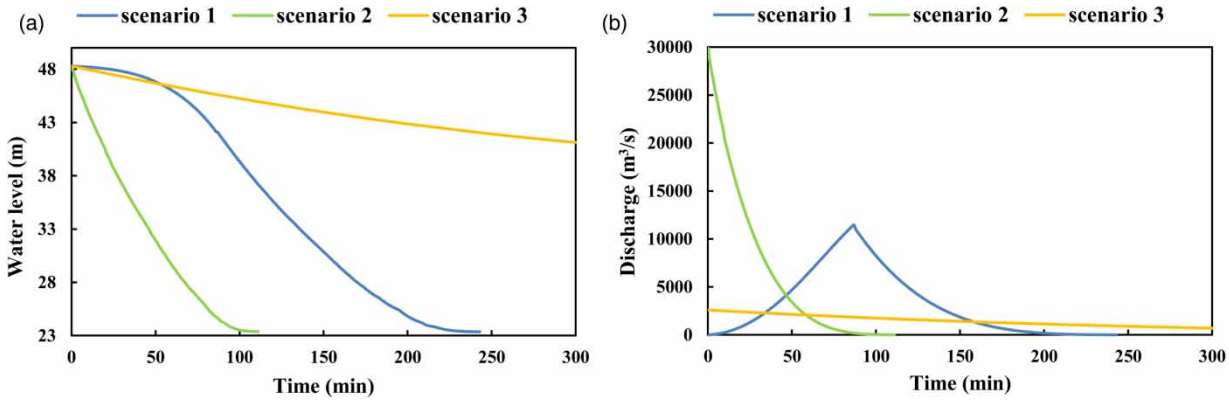

Figure 4 | Comparison of water level and discharge process for the modeled dam-break scenarios. (a) Water level; (b) Discharge.

Table 4 | Flood impact under the modeled dam-break scenarios

Scenario	Submerged area (km²)	Time to reach Pingshui Town (min)	Duration of flooding in Pingshui Town (min)	Time to reach Jishan Street (min)	Average submerged water depth in Pingshui Town (m)	Maximum submerged water depth in Pingshui Town (m)	Maximum flow velocity in Pingshui Town (m/s)
1	84.68	21	60	150	3–6	5.2	5.9
2	81.77	7	20	90	4–6.5	6.3	6.6
3	63.49	12	45	200	0.6–2.6	2.2	2.5

See Table 2 for details of each scenario

results show that all three dam-break flood Scenarios would have a direct impact on most towns and streets in Pingshui Town and Yuecheng District. The area of inundation and water depth, and the process of inundation are compared and analyzed below.

Submerged range and water depth

The simulated maximum submerged range and water depth under each scenario are mapped in Figure 5. Maximum inundation areas of 84.68, 81.77 and 63.49 km^2 occurred about 10, 8 and 11 h after dam-break in Scenarios 1, 2 and 3, respectively. Shaoxing City is sufficiently distant from Pingshuijiang Reservoir that the dense water network can absorb a large amount of incoming water; submerged areas are on both sides of the river network and water depth is relatively limited. Jishan Street, which is closest to the reservoir, is the most impacted and a large area is flooded under each scheme. In Langgang New Village near Pingshui Town, the maximum submerged depth is 1.59, 1.26 and 0.86 m in Scenarios 1, 2 and 3, respectively.

Pingshui town, located only 3.7 km downstream of the reservoir, is directly affected by flooding and the impact is potentially serious. The maximum inundation area in Scenarios 1 and 2 is roughly similar, with almost complete inundation in Pingshui Town, while that of Scenario 3 is relatively small (Figure 6). The maximum submerged area in Scenarios 1, 2 and 3 are 5.2, 6.3 and 2.2 m (Table 4), respectively, near Pingshui Street in Pingshui Town.

Submergence process

The submergence areas after 1 h for the modeled dam-break scenarios are superimposed in Figure 6(b), and changes in submergence depth near Pingshui Street in Pingshui Town over 8 h after dam-break are shown in Figure 7(a). In Scenario 1, submergence depth gradually increases after dam failure, corresponding with the flow rate, and reaches Pingshui Town after 21 min. The flow rate is faster in Scenarios 2 and 3, with Pingshui Town becoming submerged after 7 and 12 min,

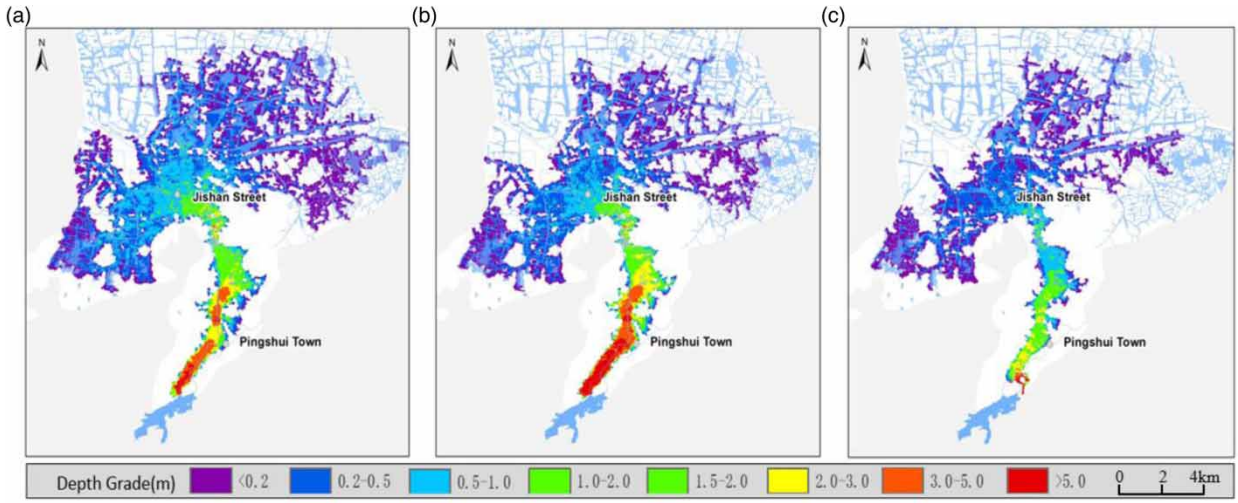

Figure 5 | Modeled maximum submerged area and water depth in each dam-break scenario. (a) Scenario 1; (b) Scenario 2; (c) Scenario 3.

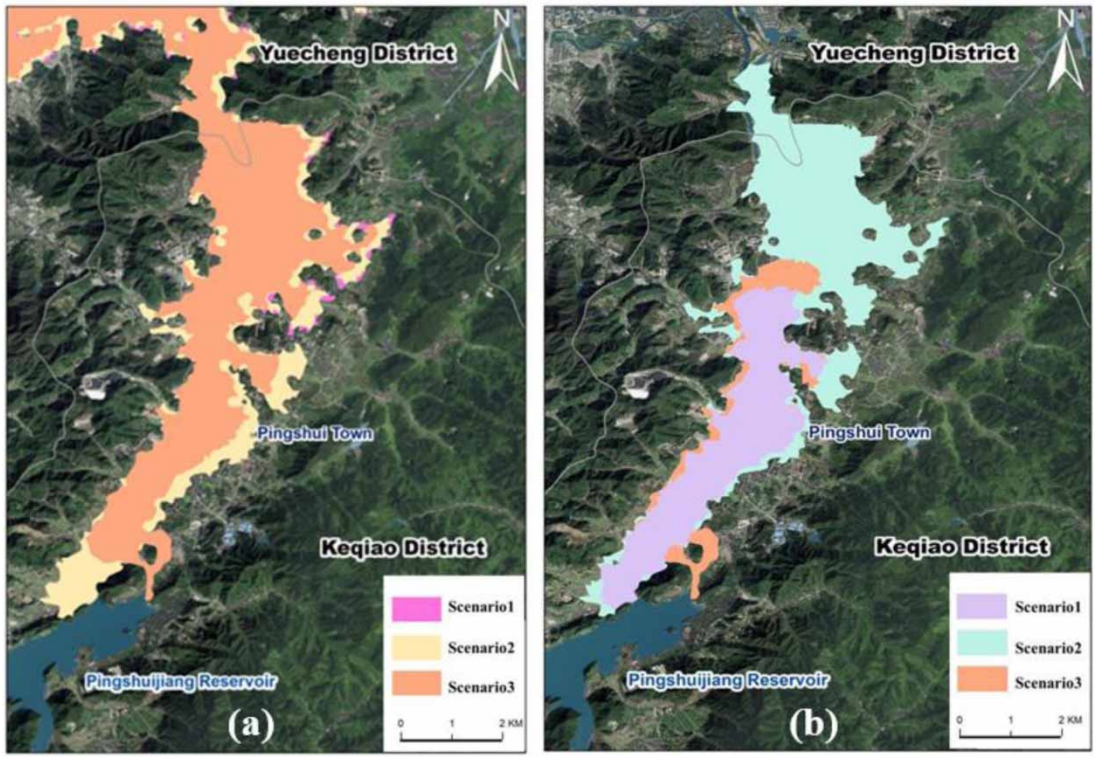

Figure 6 | Submergence area for the modeled dam-break of each scenarios. (a) Maximum submergence area. (b) Submergence area 1 h after dam-break.

respectively. The main areas of the town are flooded after 60, 20 and 45 min of dam-break, with maximum flow rates of 5.9, 6.6 and 2.5 m/s, in Scenarios 1–3, respectively.

Figure 7(b) shows changes in submergence depth over time at Jishan Street, Langgang New Village. Here, flooding commenced at 150, 90 and 200 min after dam-break in Scenarios 1–3, respectively. The maximum submerged range was reached after about 10, 8 and 11 h, respectively.

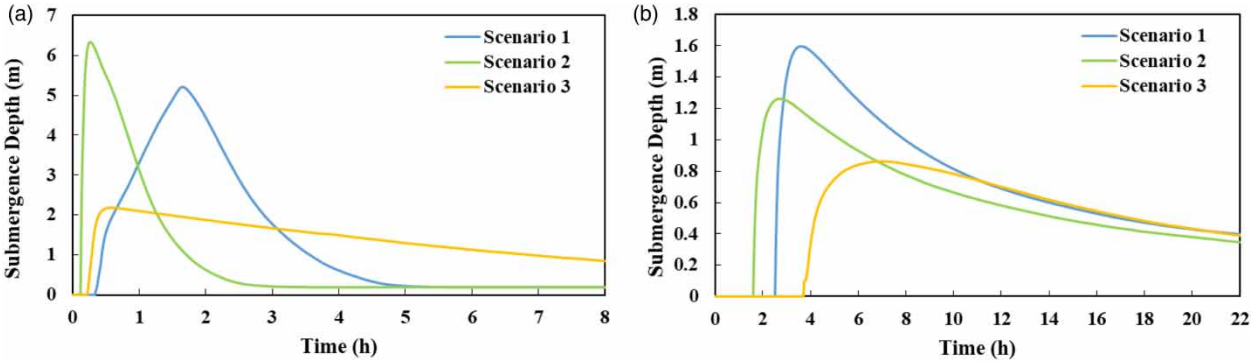

Figure 7 | Changes in submergence depth over time under the modeled dam-break scenarios. (a) Pingshui Street, Pingshui Town; (b) Jishan Street, Langgang New Village.

CONCLUSIONS

This study compares and analyzes the downstream impacts of different dam-break scenarios for Pingshuijiang Reservoir in southeastern China. The downstream flood routing process is simulated for three scenarios, with flood characteristics such as submergence depth, inundated area and arrival time calculated. Flood development dynamics and regional flood impact are evaluated, and emergency rescue conditions are analyzed. The results show significant differences in flood process and submergence under the three scenarios due to dam-break size and dam-break mode.

(1) Scenario 1 involves the gradual failure of the main dam. Though peak discharge reaches 11,440 m^3/s, which almost submerges the whole of Pingshui Town, and has a direct impact on most township streets in Yuecheng District. However, flooding occurs gradually, and submerged water depth is largely below 1 m within 30 min of dam-break, and it takes another 30 min to submerge the main area of the town. Hence, there is sufficient time to warn and evacuate people living in the affected areas.

(2) Scenario 2 involves the instantaneous complete collapse of the main dam. Peak discharge is significantly larger than in the other scenarios (30,117 m^3/s), and occurs at the beginning of the dam-break. The flood reaches Pingshui Town after 7 min and the town is submerged within 20 min. The rapidity and extent of flooding would have a devastating effect on the whole town, with no time for early warning and immediate rescue/evacuation.

(3) In Scenario 3, instantaneous failure of the auxiliary dam, peak discharge is much lower at 2,589 m^3/s due to the relatively small breach and low rate of flow. Although the flood reaches the town in 12 min and submerges the town after 45 min, the water depth is generally less than 2 m. Hence, there is ample opportunity for rescue and evacuation.

There are two shortcomings to the study that could be addressed in future work. Due to the uncertainty of upstream rainfall conditions, inflow to the reservoir during dam-break is not considered. In addition, to fully consider the impact of the most unfavorable dam-break condition, the main dam instantaneous collapse scenario was adopted; however, this scenario is extremely rare for large and medium-sized earth-rock dams.

AUTHOR CONTRIBUTIONS

X.J. conceptualized the whole article; X.J. and C.Z. developed the methodology; X.J. and J.M. wrote the original draft; C.Z. and Q.X. conducted funding acquisition; J.M. and X.J. performed the investigation; X.J. and B.F. conducted data curation; C.Z. and D.M. visualized the article; Y.Z., Q.X. and C.J.Z. wrote the original draft and the review, and edited the article. All authors have read and agreed to the published version of the manuscript.

FUNDING

This study was sponsored by the Science and Technology Development Foundation of Yellow River Institute of Hydraulic Research (Grant No. HKF202202), the National Natural Science Foundation of China (Grant Nos. U2243220, 51909100 and 52009047) and the Fundamental Research Funds for the Central Scientific Research Institute (Grant No. HKY-JBYW-2020-03).

DATA AVAILABILITY STATEMENT

All relevant data are included in the paper or its Supplementary Information.

CONFLICT OF INTEREST

The authors declare there is no conflict.

REFERENCES

Alcayna, T., Fletcher, I., Gibb, R., Tremblay, L., Funk, S., Rao, B. & Lowe, R. 2022 Climate-sensitive disease outbreaks in the aftermath of extreme climatic events: a scoping review. *One Earth* **5** (4), 336–350.

Ali, E. B., Imane, T., Ayoub, N. & Abdeslam, T. 2022 A practical probabilistic approach for simulating life loss in an urban area associated with a dam-break flood. *International Journal of Disaster Risk Reduction* **76** (01), 97–108.

Alvarez, M., Puertas, J., Peña, E. & Bermúdez, M. 2017 Two-dimensional dam-break flood analysis in data-scarce regions: the case study of Chipembe Dam, Mozambique. *Water* **9** (6), 432.

Bai, S. N. & Zhen, Z. S. 2014 Study on the seepage defect at the connection of the overflow dam and the earth dam of Banqiao Reservoir. *Advanced Materials Research* **3465**, 287–291.

Cai, S. J., Zhang, D. & Zong-Zhi, W. U. 2011 Discussion on fuzzy risk assessment method of tailings reservoir dam-break under seismic conditions. *Journal of Safety Science and Technology* **7** (07), 10–14. (In Chinese).

Chen, H. & Sun, J. 2021 Anthropogenic influence has increased climate extreme occurrence over China. *Science Bulletin* **66** (8), 749–752.

Delenne, C., Cappelaere, B. & Guinot, V. 2012 Uncertainty analysis of river flooding and dam failure risks using local sensitivity computations. *Reliability Engineering and System Safety* **107**, 171–183.

Duffaut, P. & Larouzée, J. 2019 Geology, engineering and humanities: three sciences behind the Malpasset dam failure (France, 2 December 1959). *Quarterly Journal of Engineering Geology and Hydrogeology* **52** (4), 445–458.

Enea, A., Urzică, A. & Breabăn, I. G. 2018 Remote sensing, GIS and HEC-RAS techniques, applied for flood extent validation, based on landsat imagery, lidar and hydrological data. Case study: Baseu river, Romania. *Journal of Environmental Protection and Ecology* **19**, 1091–1101.

Guo, H. M., Hai-Song, H. U., Wen-Bing, H. U., Zhang, T.-T. & Zhang, S.-M. 2019 Hydraulic experimental study on concrete dam-break with different break modes. *Journal of Yangtze River Scientific Research Institute* **36** (01), 60–63. (In Chinese).

Khoshkonesh, A., Asim, T., Mishra, R., Dehrashid, F. A., Heidarian, P. & Nsom, B. 2022 Study the effect of obstacle arrangements on the dam-break flow. *International Journal of Comadem* **25** (1), 41–45.

Li, Z., Huangfu, Y., Li, Y., Ying, Y. & Huangfu, Z. 2021 Numerical simulation of dam-break flood in Qianping Reservoir based on BIM + GIS technology. *Yellow River* **43** (04), 160–164. (In Chinese).

Mao, J., Wang, S., Ni, J., Xi, C. & Wang, J. 2017 Management system for dam-break hazard mapping in a complex basin environment. *ISPRS International Journal of Geo-Information* **6** (6), 162.

Mudashiru, R. B., Sabtu, N., Abustan, I. & Waheed, B. 2021 Flood hazard mapping methods: a review. *Journal of Hydrology* **603** (A), 1–30.

Pradel, D. & Lobbestael, A. 2021 Edenville and Sanford dam failures: field reconnaissance report. *American Society of Civil Engineers* **2** (1), 1–8.

Pradel, D., Wartman, J. & Tiwari, B. 2017 Failure of the Fujinuma dams during the 2011 Tohoku Earthquake. *INCOLD Journal (A Half Yearly Technical Journal of Indian Committee on Large Dams)* **6** (1), 47–54.

Qiu, W., Li, Y., Wen, L. & Bu, P. 2021 Study on numerical simulation method of overtopping dam-break of concrete faced sand-gravel dam. *IOP Conference Series: Earth and Environmental Science* **783** (1), 1–6.

Safarzadeh, A. 2017 Three dimensional hydrodynamics of sudden dam-break in curved channels. *Modares Civil Engineering Journal* **17** (3), 77–88.

Seiya, W., Shintaro, F. & Changhong, H. 2021 Numerical simulation of dam-break flow impact on vertical cylinder by cumulant lattice Boltzmann method. *Journal of Hydrodynamics* **33**, 185–194.

Seyedashraf, O., Mehrabi, M. & Akhtari, A. A. 2018 Novel approach for dam-break flow modeling using computational intelligence. *Journal of Hydrology* **559**, 1028–1038.

Tamm, O. & Tamm, T. 2020 Verification of a robust method for sizing and siting the small hydropower run-of-river plant potential by using GIS. *Renewable Energy* **155**, 153–159.

Tedla, M. G., Cho, Y. & Jun, K. 2021 Flood mapping from dam-break due to peak inflow: a coupled rainfall–runoff and hydraulic models approach. *Hydrology* **8** (2), 89–89.

Weilian, L., Jun, Z., Henrik, H. J., Lin, F., Qing, Z. & Youness, D. 2022 Three-dimensional virtual representation for the whole process of dam-break floods from a geospatial storytelling perspective. *International Journal of Digital Earth* **15** (1), 104–117.

Xu, S., Chai, Y., Yue, Y., Yan, X. & Zhang, X. 2021 Seasonal changes of sediment fluxes in the Yangtze River: roles of precipitation change, human conservation measures in sub-basins, and large dams. *Hydrology Research* **52** (2), 461–477.

First received 30 November 2022; accepted in revised form 16 January 2023. Available online 2 February 2023